arXiv:1403.3318v2 [hep-lat] 14 Oct 2014

IFT-UAM/CSIC-14-014

The Continuum Phase Diagram of the 2d Non-Commutative $\lambda\phi^4$ Model

Héctor Mejía-Díaz[a], Wolfgang Bietenholz[a] and Marco Panero[b]

[a] Instituto de Ciencias Nucleares
Universidad Nacional Autónoma de México
A. P. 70-543, C. P. 04510 Distrito Federal, Mexico

[b] Instituto de Física Teórica UAM/CSIC
Universidad Autónoma de Madrid
Ciudad Universitaria de Cantoblanco
28049 Madrid, Spain

We present a non-perturbative study of the $\lambda\phi^4$ model on a non-commutative plane. The lattice regularised form can be mapped onto a Hermitian matrix model, which enables Monte Carlo simulations. Numerical data reveal the phase diagram; at large λ it contains a "striped phase", which is absent in the commutative case. We explore the question whether or not this phenomenon persists in a Double Scaling Limit (DSL), which extrapolates simultaneously to the continuum and to infinite volume, at a fixed non-commutativity parameter. To this end, we introduce a dimensional lattice spacing based on the decay of the correlation function. Our results provide evidence for the existence of a striped phase even in the DSL, which implies the spontaneous breaking of translation symmetry. Due to the non-locality of this model, this does not contradict the Mermin-Wagner theorem.

1 Introduction

Since the dawn of the new millennium, field theory on non-commutative spaces ("NC field theory") has attracted a lot of interest, see Refs. [1, 2] for reviews. The idea as such is historic [3], but the observation that it can be related to low energy string theory [4] triggered an avalanche of thousands of papers on this subject.

The point of departure are space-time coordinates, which are given by Hermitian operators that do not commute. In the functional integral approach, however, NC field theory can be formulated with ordinary space-time coordinates x, if the field multiplications are carried out using the Moyal star-product,

$$\phi(x) \star \psi(x) := \phi(x) \exp\Big(\frac{\mathrm{i}}{2} \overleftarrow{\partial}_\mu \Theta_{\mu\nu} \overrightarrow{\partial}_\nu\Big)\psi(x) \ . \tag{1.1}$$

In particular the star-commutator of the coordinates,

$$x_\mu \star x_\nu - x_\nu \star x_\mu = \mathrm{i}\Theta_{\mu\nu} \ , \tag{1.2}$$

yields the (real, anti-symmetric) non-commutativity "tensor" Θ. Here we consider the simplest case, where Θ is constant.

The perturbative treatment of NC field theory is obstructed by the notorious problem of mixing between ultraviolet and infrared (UV/IR) degrees of freedom, *i.e.* the appearance of singularities at both ends of the energy scale in non-planar diagrams [5]. Therefore, renormalisation beyond one loop is mysterious. Effects due to this mixing also show up at the non-perturbative level, as this study is going to confirm.

In quadratic, integrated terms (with vanishing boundary contributions) the star-product is equivalent to the ordinary product. Hence the Euclidean action of the NC $\lambda\phi^4$ model takes the form[1]

$$S[\phi] = \int d^d x \left[\frac{1}{2}\partial_\mu\phi\,\partial_\mu\phi + \frac{m^2}{2}\phi^2 + \frac{\lambda}{4}\phi\star\phi\star\phi\star\phi\right] \ , \tag{1.3}$$

so λ does not only control the strength of the coupling, but also the extent of the non-commutativity effects.

A 1-loop calculation in the framework of a Hartree-Fock approach led to the following conjecture about the phase diagram of this model in $d = 3$ and

[1] As usual, the energy dimension of ϕ is $(d-2)/2$ and the dimension of the quartic coupling λ is $(4-d)$.

4 [6]: there is a disordered phase, and — at strongly negative m^2 — an order regime. The latter splits into a phase of uniform magnetisation (at small λ, with an Ising-type transition to disorder, as in the commutative case), and a "striped phase" (at large λ), where periodic non-uniform magnetisation patterns dominate. That phase, which does not exist in the commutative $\lambda\phi^4$ model, was also discussed based on renormalisation group methods [7] and on the Cornwall-Jackiw-Tomboulis effective action [8]. In $d = 3$, more precisely in the case of a NC plane and a commutative Euclidean time direction, the existence of such a striped phase was observed explicitly in a non-perturbative, numerical study on the lattice [9], in agreement with the qualitative prediction of Ref. [6].

The numerical computation of the dispersion relation $E = E(\vec{p})$ (with $\vec{p} = (p_1, p_2)$) revealed that for λ values above some critical $\lambda_{\rm c}$, the energy E grows not only at large momenta, but also at very small $|\vec{p}|$, hence E takes its minimum at some finite momentum. A strongly negative parameter m^2 enforces ordering with the pattern corresponding to the modes of minimal energy: this results in a (Poincaré symmetry breaking) type of order which can be defined as a "stripe pattern". The momentum value corresponding to the minimum E stabilises as one approaches a Double Scaling Limit (DSL), *i.e.* by taking the continuum (lattice spacing $a \to 0$) and thermodynamic (physical volume and number of degrees of freedom tending to infinity) limits, at fixed non-commutativity tensor [9]. This shows that the striped phase does indeed exist in $d = 3$, which is a manifestation of the coexistence of UV and IR divergences. In addition, it also suggests non-perturbative renormalisability.

Such a striped phase was also observed numerically in the 2d lattice model [9,10], but the survival of that phase in the DSL has never been clarified. One might suspect that it does not survive this limit, *i.e.* that the DSL removes the phase boundary inside to ordered regime, $\lambda_{\rm c} \to \infty$, because in such a phase translation and rotation symmetry are spontaneously broken. Indeed, in lattice field theory there exist phases, which are regularisation artifacts, such as the confinement phase in lattice Quantum Electrodynamics at strong coupling. Naïvely, one could think that the persistence of the striped phase in the continuum limit would violate the Mermin-Wagner theorem [11], which rules out the spontaneous breaking of continuous, global symmetries in $d \leq 2$. However, this theorem is based on assumptions like locality and a regular IR behaviour, which do not hold here, and hence it is not automatically applicable in NC field theory.

Therefore Ref. [6] presented a refined consideration, and conjectured the absence of a striped phase in $d = 2$. The authors argued based on an effective action of the Brazovskii form: in this formulation, the kinetic term is of fourth order in the momentum, which renders the statement of the Mermin-Wagner theorem more powerful. This suggests that it might even capture the NC case. On the other hand, another effective action approach supported the existence of a striped phase in $d = 2$ [12].

Here we investigate this controversial question numerically; this has been reported before in a thesis and in a proceeding contribution [13]. In Section 2 we review the matrix model formulation; in this form, the model is tractable by Monte Carlo simulations. Section 3 describes the phase diagram on the lattice. Section 4 introduces a physical scale in order to address the question if there exists a stable DSL in the vicinity of the striped phase. We summarise our conclusions in Section 5. Some numerical tricks, which are useful in the simulation of Hermitian matrix models, are sketched in Appendix A.

2 Formulation on the lattice and as a matrix model

As relation (1.2) shows, the points on a non-commutative plane are somewhat washed out, hence it is not possible to discretise a non-commutative plane by means of a lattice with sharp sites. On the other hand, the momentum components are assumed to commute with each other. As suggested in Refs. [2, 18], a (fuzzy) lattice structure can be introduced, by restricting the momenta of the NC theory to the first Brillouin zone. This is only consistent for discrete momenta, hence the NC lattice is automatically periodic. In particular, on a periodic $N \times N$ lattice of spacing a, the non-commutativity parameter θ is identified as

$$\theta = \frac{1}{\pi} N a^2 \ , \qquad \text{with} \quad \Theta_{\mu\nu} = \theta \epsilon_{\mu\nu} \ . \tag{2.1}$$

The DSL consists of the simultaneous limits $N \to \infty$ and $a \to 0$ at $Na^2 =$ const., *i.e.* one extrapolates to the continuum and to infinite volume (since Na also diverges), while keeping the non-commutativity parameter θ constant.

However, such a formulation is still unpractical for numerical simulations, because the star-product couples field variables defined on *any* pair of lat-

tice sites. Fortunately, a computer-friendly formulation can be obtained by mapping the system to a twisted matrix model. Such a mapping was first suggested in the context of NC $U(N)$ gauge theory [19] (in which twisted boundary conditions are required for the algebra to close).[2] Similarly, the matrix formulation of the NC $\lambda\phi^4$ model takes the form [18]

$$S[\Phi] = N\mathrm{Tr}\left[\frac{1}{2}\sum_{\mu=1}^{2}\left(\Gamma_\mu\Phi\Gamma_\mu^\dagger - \Phi\right)^2 + \frac{\bar{m}^2}{2}\Phi^2 + \frac{\bar{\lambda}}{4}\Phi^4\right] , \tag{2.2}$$

where Φ is a Hermitian $N \times N$ matrix, which captures in one point all the degrees of freedom of the lattice field, while $\bar{m}^2$ and $\bar{\lambda}$ are the (dimensionless) parameters of the matrix model, expressed in units of the lattice spacing a. The Γ_μ are unitary matrices called *twist eaters*: they satisfy the 't Hooft-Weyl algebra

$$\Gamma_\mu\Gamma_\nu = \mathcal{Z}_{\nu\mu}\Gamma_\nu\Gamma_\mu , \tag{2.3}$$

where the $\mathcal{Z}$ tensor encodes the twist factor in the boundary conditions. We choose $\mathcal{Z}_{12} = \mathcal{Z}_{21}^* = \exp\left[\mathrm{i}\pi(N+1)/N\right]$, where the matrix (or lattice) size N has to be odd. This choice, and the form of the twist eaters corresponding to "shift" and "clock" matrices,

$$\Gamma_1 = \begin{pmatrix} 0 & 1 & 0 & . & . & 0 \\ 0 & 0 & 1 & . & . & . \\ 0 & 0 & 0 & . & . & . \\ . & . & . & . & . & . \\ . & . & . & . & 0 & 1 \\ 1 & . & . & . & 0 & 0 \end{pmatrix} \quad , \quad \Gamma_2 = \begin{pmatrix} 1 & 0 & 0 & . & . & 0 \\ 0 & \mathcal{Z}_{21} & 0 & . & . & . \\ 0 & 0 & \mathcal{Z}_{21}^2 & . & . & . \\ . & . & . & . & . & . \\ . & . & . & . & \mathcal{Z}_{21}^{N-2} & 0 \\ 0 & . & . & . & 0 & \mathcal{Z}_{21}^{N-1} \end{pmatrix}$$

follows Refs. [9, 18], and is similar to the formulation in Ref. [10].

This type of matrix model has also been studied in Ref. [20], which further supported the scenario of a striped phase phase in $d = 2$ and 4. Moreover, the formulation of the $\lambda\phi^4$ model on a "fuzzy sphere" also leads to NC coordinates on the regularised level, though they obey a different non-commutativity relation, where $\Theta(x)$ is not constant. Also that model can be translated into

[2] Large-N Yang-Mills theories defined on a space with twisted boundary conditions were first introduced in Ref. [14] and used in simulations of NC gauge theories [15]; see also Subsection 4.7 of Ref. [16] for an introduction to this subject, and Ref. [17] for recent applications.

a Hermitian matrix formulation similar to eq. (2.2), which has been studied numerically in $d = 2$ [21] and in $d = 3$ [22]. As a further variant, Ref. [23] studied the $\lambda\phi^4$ model on a fuzzy cylinder. In all these cases, the phase diagram at finite N involves a striped phase as well.

3 The phase diagram on the lattice

Figure 1 shows the phase diagram obtained from our Monte Carlo simulations of this model, in its matrix formulation (2.2).[3] The qualitative features of the phase diagram agree with those in $d = 3$ [6]. There is a disordered phase at positive or weakly negative m^2; when this parameter decreases below some critical value $m_{\rm c}^2(\lambda) < 0$, the disordered phase gives way to an order regime. At small λ this order is uniform, but at larger λ it is "striped", *i.e.* the ground state breaks the rotational and translational symmetries of the system. The precise location of the boundary between the uniform- and non-uniform-order phases is particularly challenging to identify, hence the dotted vertical line in Figure 1 is only suggestive.

On the other hand, the boundary between the disordered and the ordered phases can be identified well, as described below. To a very good accuracy, its location stabilises for $N \gtrsim 19$, if the phase diagram is plotted as a function of $N^{3/2}m^2$ and $N^2\lambda$. Note that this differs from the 3d case, where the choice of axes making the scaling properties manifest is N^2m^2 and $N^2\lambda$ [9]. In $d = 2$, in the limit of very large quartic couplings — in which the kinetic term (in the matrix formulation) becomes negligible — the theory reduces to a one-matrix model, for which the boundary of the disordered phase is given by $\bar{m}_{\rm c}^2 = -2\sqrt{\lambda}$ [24]. This behaviour was confirmed numerically in the related fuzzy sphere model [21], but it is not visible in Figure 1, which does not extend to very large values of λ.

The phase diagram in Figure 1 can be divided into four sectors, depending whether $N^2\lambda$ and $-N^{3/2}m^2$ are small or large. For each of these sectors, a typical configuration is shown in Figure 2. These figures are obtained by mapping the $N \times N$ matrices back to a scalar field configuration, according to the prescription in Refs. [18] (the Φ_x values correspond to bright or dark spots, according to the colour code on the right-hand-side).

[3] For simplicity, throughout this section all dimensional quantities are expressed in lattice units.

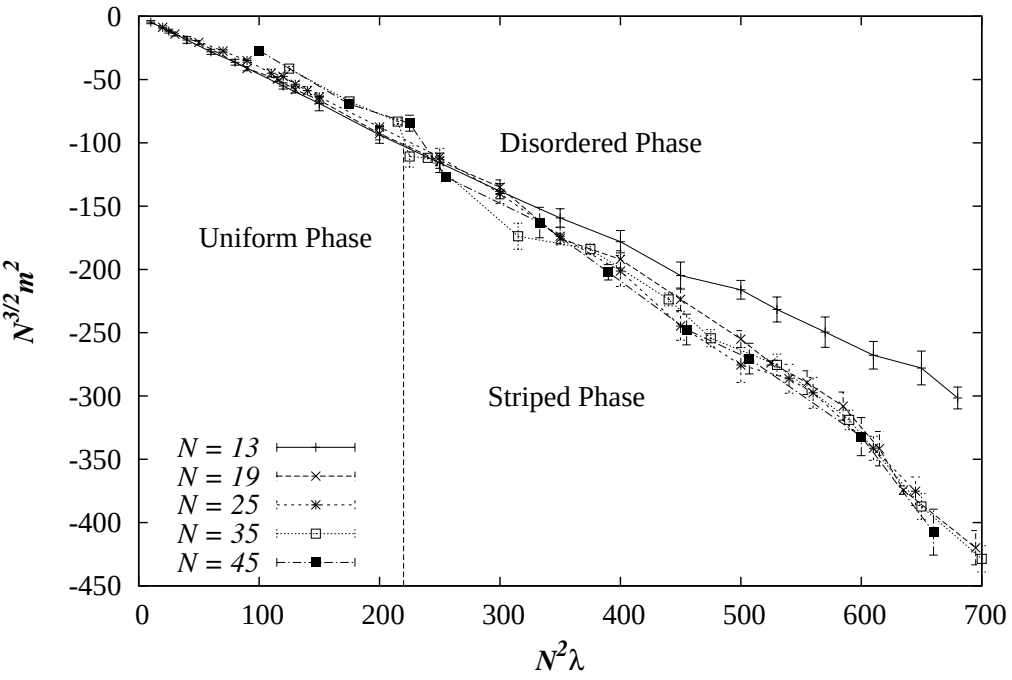

Figure 1: The phase diagram of the 2d NC $\lambda\phi^4$ model. The lattice size is $N \times N$, and a stable phase transition line between order and disorder is observed for $N \geq 19$. At small coupling λ this order is uniform, but at large λ, where NC effects are no longer negligible, it becomes striped. (The quantities on both axes are expressed in units of a^{-2}.)

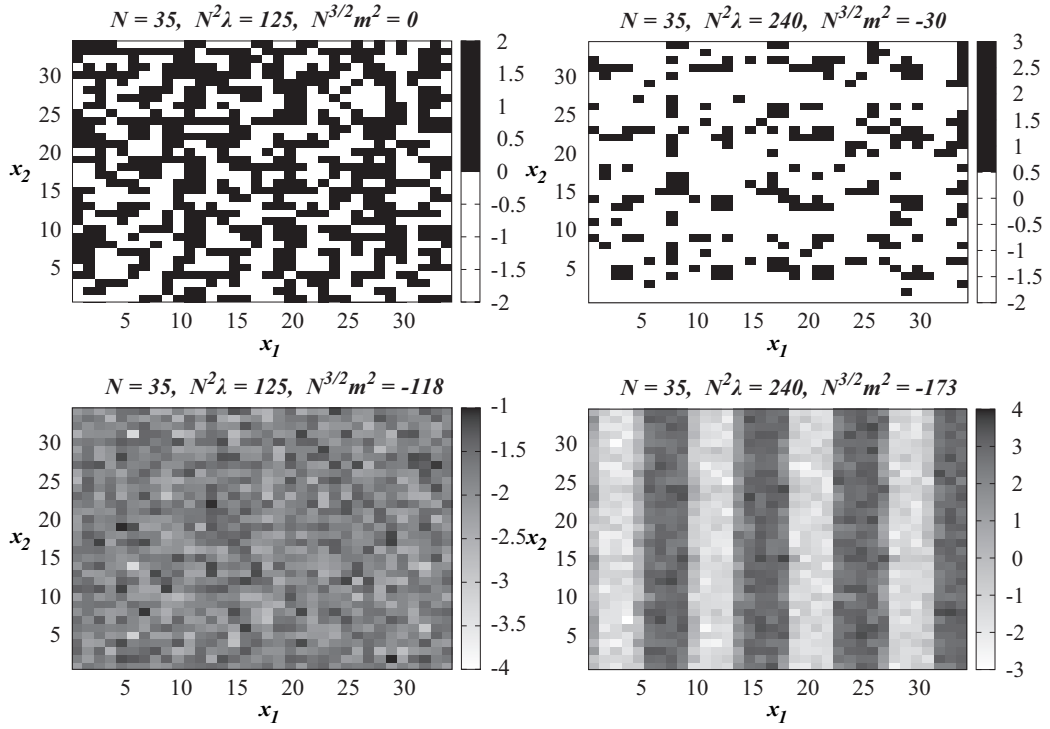

Figure 2: An illustration of typical configurations in the four sectors of the phase diagram shown in Figure 1. The upper plots are in the disordered phase, next to the uniform phase (on the left) and to the striped phase (on the right). The lower plots show examples of uniform and of striped ordering.

We add an analogous consideration of the propagator in momentum space,[4]

$$G(\vec{p}) = \langle \tilde{\phi}(-\vec{p})\, \tilde{\phi}(\vec{p}) \rangle = G\left(\tfrac{2\pi}{N}\vec{k}\right) \;, \quad \tilde{\phi}(\vec{p}) = \frac{1}{N^2} \sum_{\vec{x}} \phi_{\vec{x}}\, e^{-\mathrm{i}\,\vec{p}\cdot\vec{x}} \;. \tag{3.1}$$

The momentum space propagator also played an essential rôle in the analysis of Ref. [6]. It is worth noting, however, that certain properties characterising the propagator in a commutative theory do not trivially extend to the NC case. For example, the interpretation in terms of a spectral representation is

[4]For convenience, the momentum $\vec{p}$ is re-scaled to $\vec{k} = \frac{N}{2\pi}\vec{p}$, since the stripe patterns correspond to integer components k_μ.

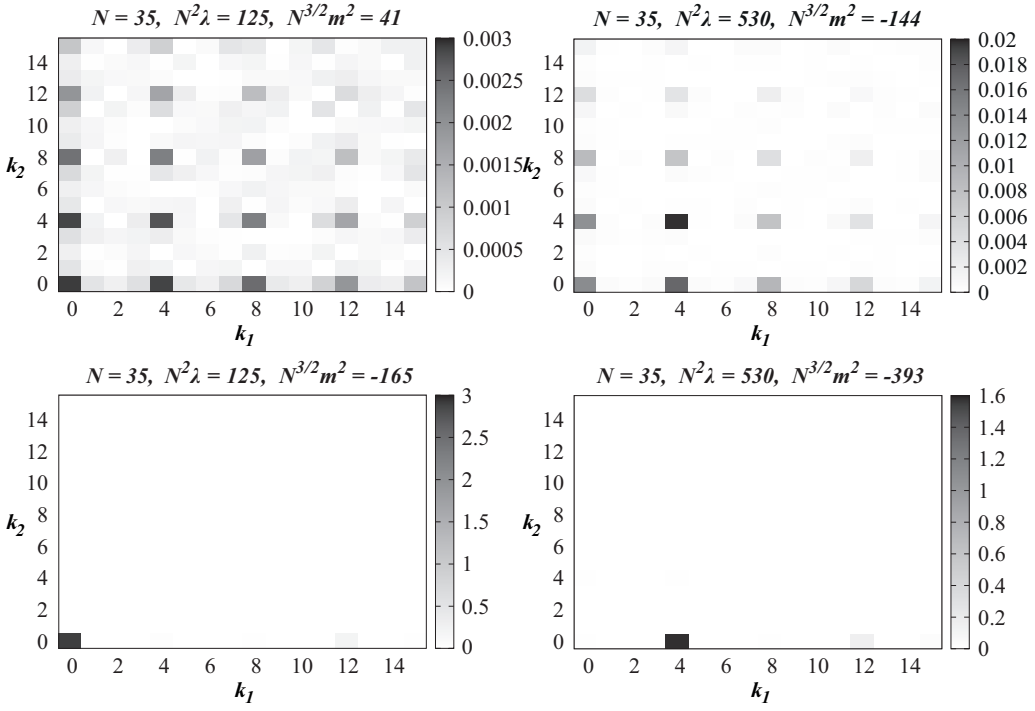

Figure 3: Another illustration of typical configurations in the four sectors of the phase diagram shown in Figure 1. Here we show typical contributions to the momentum space propagator $G(\vec{k})$ (cf. eq. (3.1)) at specific parameters m^2 and λ. The upper plots are in the disordered phase, next to the uniform phase (on the left) and to the striped phase (on the right). The lower plots show examples of uniform and of striped ordering.

subtle, and the meaning of the energy eigenvalues in the case when the non-commutativity involves the (Euclidean) time coordinate is delicate. However, our considerations are not affected by these questions.

Figure 3 shows another set of maps in the four sectors of the phase diagram, where now the brightness/darkness indicate the value of $G(\vec{k})$ in the (k_1, k_2) plane. These maps correspond to the $G(\vec{k})$-contributions of typical configurations, which fully confirm the picture of Figure 2.

To identify these different phases systematically, we computed the expectation values of a set of suitable momentum-dependent order parameters $M(k)$. For a given absolute value of $k = |\vec{k}|$, and a given field configuration,

the value of $M(k)$ is defined as the maximum of the modulus of the Fourier transform of Φ_x,

$$M(k) = \frac{1}{N^2} \max_{\frac{N}{2\pi}|\vec{p}|=k} \left| \sum_x e^{-i\vec{p}\cdot\vec{x}} \Phi_x \right| . \tag{3.2}$$

According to this definition, $M(k=0)$ reduces to the standard order parameter for uniform magnetisation (and the normalisation is such that it equals the average value of Φ_x on a given configuration). On the other hand, for non-zero k this observable can detect a possible dominance of striped patterns (the stripes are maximally manifest orthogonally to the $\vec{k}$-direction, which is summed over in $\langle M(k) \rangle$).

Figure 4 shows examples how the order parameters $\langle M(0) \rangle$ or $\langle M(4) \rangle$ become significant for decreasing m^2.

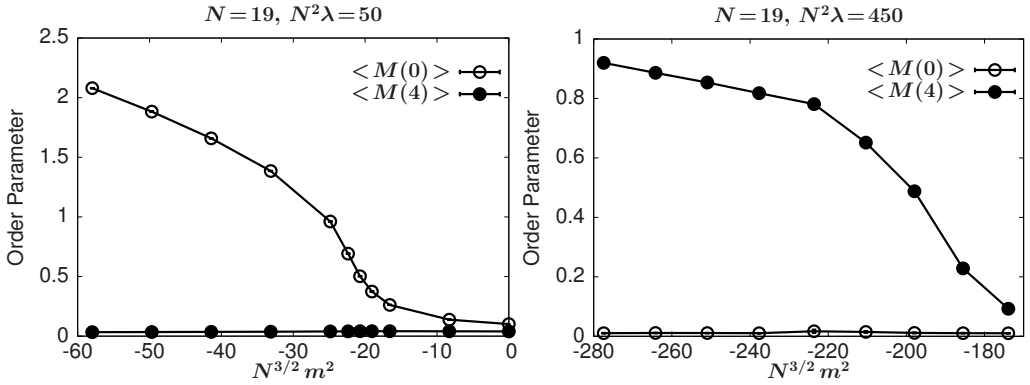

Figure 4: The order parameters $\langle M(0) \rangle$ and $\langle M(4) \rangle$, which are defined in eq. (3.2). The figures show the dependence on m^2 at fixed N and λ. For small (large) λ and decreasing m^2, the disorder turns into a uniform (4-stripe) pattern.

Again we add analogous results for the propagator in momentum space. Figure 5 shows the expectation values $G(k)$ for the relevant values of k, as a function of m^2, at fixed λ. Also here we observe a behaviour which is entirely consistent with the one of $\langle M(k) \rangle$, namely the onset of $G(0,0)$ (of $G(4,0)$ or $G(0,4)$) as m^2 decreases down to the uniform (striped) phase. At the largest λ-value in this set (plot on the bottom, right), we also see some imprint of $G(4,4)$, *i.e.* here also the contribution of a "checkerboard-type" pattern is

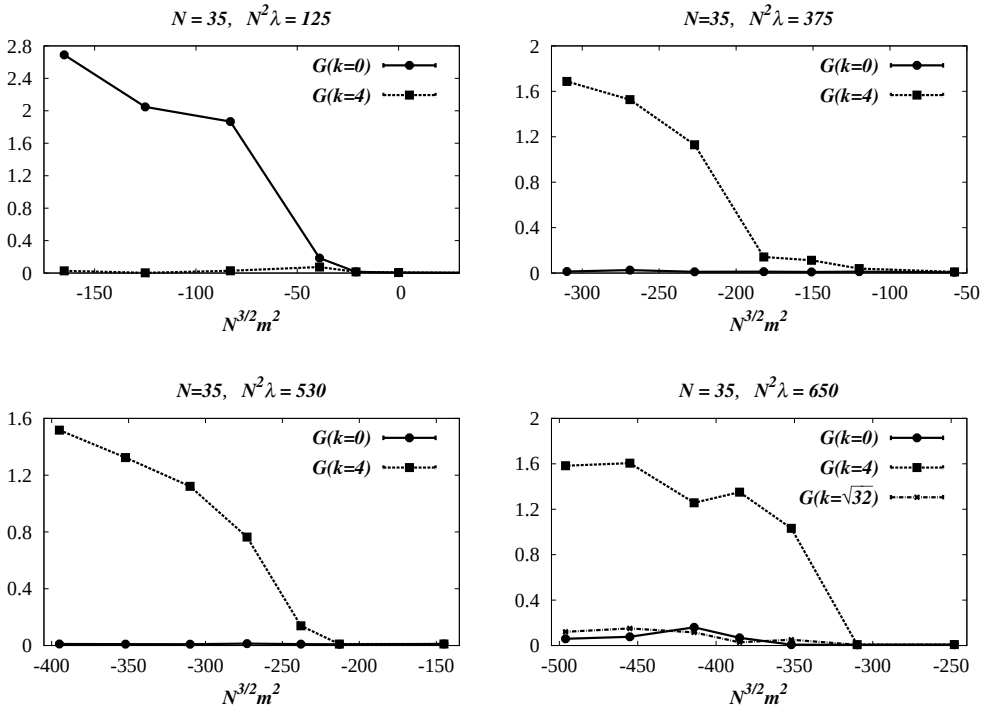

Figure 5: The momentum space propagator $G(k)$ (cf. eq. (3.1), and $k = |\vec{k}|$) at $N = 35$ and fixed λ, as a function of m^2. As m^2 decreases, we confirm the phase transition to an ordered phase: for small λ to the uniform phase (top, left), and for larger λ to the striped phase (remaining three plots). At large λ we also notice a non-negligible contribution of $G(\vec{k} = (4, 4))$.

not negligible anymore.

Such pictures reveal the type of emerging order unambiguously, but for the identification of the critical value m_c^2 it is favourable to consider the connected correlation function of the relevant order parameter,

$$\langle M(k)^2 \rangle_{\rm conn} = \langle M(k)^2 \rangle - \langle M(k) \rangle^2 \ . \tag{3.3}$$

Here the transition corresponds to a peak, which can be located well, as the examples in Figure 6 show. This property also shows that these order-disorder phase transitions are of second order.

At low λ, this is an Ising-type transition, which also occurs in the com-

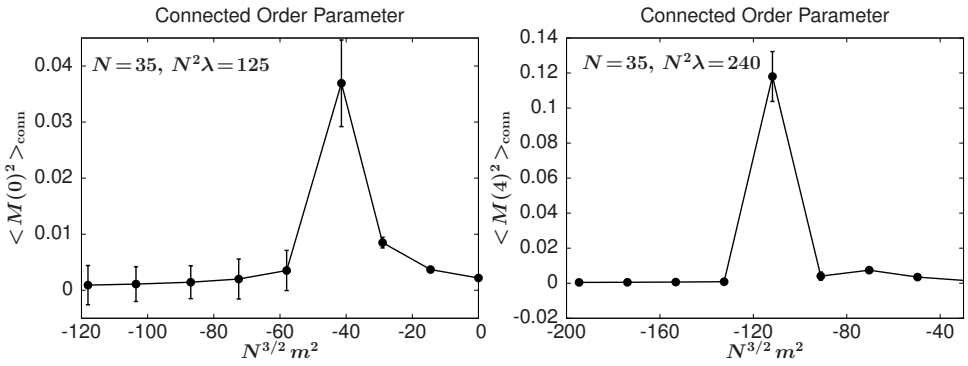

Figure 6: The connected correlation function of the order parameters $\langle M(0)^2\rangle_{\rm conn}$ and $\langle M(4)^2\rangle_{\rm conn}$. In both cases they exhibit a rather sharp peak, which allows us to identify the critical value $m_{\rm c}^2$.

mutative $\lambda\phi^4$ model, as argued in Ref. [6]. Regarding the transition to the striped phase it should be noted, however, that the correlation function does not decay exponentially, hence it is not possible to extract a correlation length. An example for the correlation function in the disordered phase, but close to striped ordering, is shown in Figure 7. The trend towards a 4-stripe pattern, which condenses at somewhat lower m^2, is clearly visible.

Also in the 3d case non-exponential correlations were observed within the NC plane [9]. However, in that case the decay was exponential in the third (commutative) direction, which did provide a correlation length, along with the aforementioned dispersion relation $E(\vec{p})$.

4 The Double Scaling Limit

So far, the discussion of our results has been in terms of quantities expressed in lattice units. In order to discuss the DSL, however, it is necessary to introduce a dimensional quantity to "set the scale" and to be able to take the continuum limit. In particular, a question of central relevance in our analysis is whether the DSL can be taken while remaining in the proximity of the striped phase: if this is the case, it provides a piece of evidence for the persistence of that phase in the continuum theory at fixed non-commutativity parameter.

Since the correlation function does not decay exponentially, it is not possible to resort to the standard procedure, which refers to the correlation length

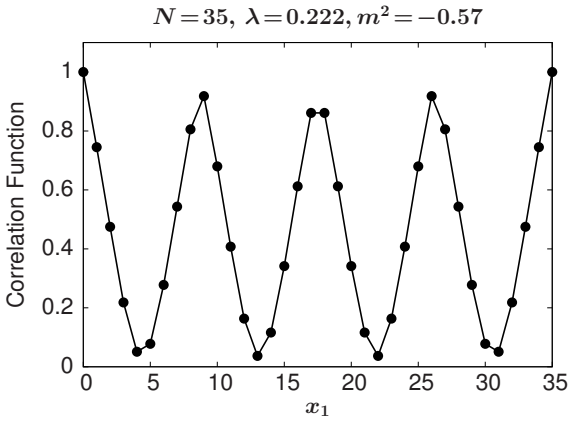

Figure 7: The correlation function $\langle \phi_{(0,0)} \phi_{(x_1,0)} \rangle$ in the point $(N^2\lambda, N^{3/2}m^2) = (272, -118)$, which is disordered, but close to the transition to the striped phase. The figure reveals a trend towards the 4-stripe pattern, which sets in at somewhat lower m^2. (We normalised the correlation function such that $\langle \phi_{\vec{x}} \phi_{\vec{x}} \rangle = 1$.)

as the natural "physical" scale. Nevertheless, an appropriate physical scale can be extracted from the decay of the correlation function, which becomes a slowly varying function of the distance when m^2 approaches m_c^2. To suppress finite size effects, we consider the limit

$$\Delta m^2 := m^2 - m_{\rm c}^2 \ \to \ 0 \tag{4.1}$$

from above, *i.e.* within the disordered phase. The goal is to increase N at the same time, in such a way that the correlation function remains stable down to the first dip. Thus Δm^2 will be converted into the factor needed for the DSL, with a critical exponent that we denote as σ,

$$a^2 \propto (\Delta m^2)^\sigma \ , \tag{4.2}$$

and which remains to be determined.

As a normalisation, we choose the units such that $a = 1$ at $N = 35$, which means that distances take the form

$$a\vec{x} = \sqrt{\frac{35}{N}}\vec{x} \ , \tag{4.3}$$

if we keep Na^2 fixed, as required for the DSL. We relate this term to Δm^2 as

$$Na^2 = N\frac{(\Delta m^2)^\sigma}{(m_{\rm c}^2)^{1+\sigma}} \ . \tag{4.4}$$

This is an ansatz, which is consistent with the proportionality relation (4.2), and which expresses the distance from the continuum limit in terms of a dimensionless ratio (much in the spirit of the dimensionless temperature $\tau := (T - T_{\rm c})/T_{\rm c}$, or the dimensionless pressure, often used to parameterise the vicinity of a phase transition in thermal statistical mechanics). More explicitly, the right-hand side of eq. (4.4) accounts for the fact that Na^2 has energy dimension -2, so the suppression factor to the trivial proportionality relation $Na^2 \propto N/m_{\rm c}^2$ depends on a dimensionless ratio, like $\Delta m^2/m_{\rm c}^2$.

The practical method to determine σ proceeds as follows: we consider two sizes N_1 and N_2, and we search for the parameters which correspond to the same trajectory towards the DSL. Hence we fix the same coupling λ, so that the dimensionless product $\lambda\theta$ is kept constant. Then we adjust values of Δm_1^2 and Δm_2^2, in such a manner that the correlation decays coincide (as well as possible) until the first dip is reached. Figure 8 shows examples for such "matched correlations functions" at three values of λ, and various sizes in each case.

Having identified such pairs Δm_1^2, Δm_2^2 — and the corresponding critical values $m_{1,{\rm c}}^2$, $m_{2,{\rm c}}^2$ — we extract the critical exponent

$$\sigma = \frac{\ln(m_{1,{\rm c}}^2/m_{2,{\rm c}}^2)}{\ln(\Delta m_1^2/\Delta m_2^2) + \ln(m_{1,{\rm c}}^2/m_{2,{\rm c}}^2)} \ . \tag{4.5}$$

This can be done for various pairs N_1, N_2, at fixed λ, always in the vicinity of the striped phase. In practice, the accessible values of $N^2\lambda$ are restricted by the feasibility of the simulation: for $N_1 < N_2$ the value of λ has to be large enough for $N_1^2\lambda$ to be close to the striped phase, but $N_2^2\lambda$ should not become too large, to avoid a situation with a multitude of deep meta-stable minima, where the Monte Carlo history could get stuck. On the other hand, N_1 and N_2 should differ significantly — and both should be large enough to attain the asymptotic large-volume regime — for the results for the σ exponents to be sensible.

If these results stabilise for increasing N_1, N_2 and decreasing Δm_1^2, Δm_2^2, we can conclude that it is indeed possible to take a DSL next to the striped phase, so that the latter persists — otherwise it would likely be removed in

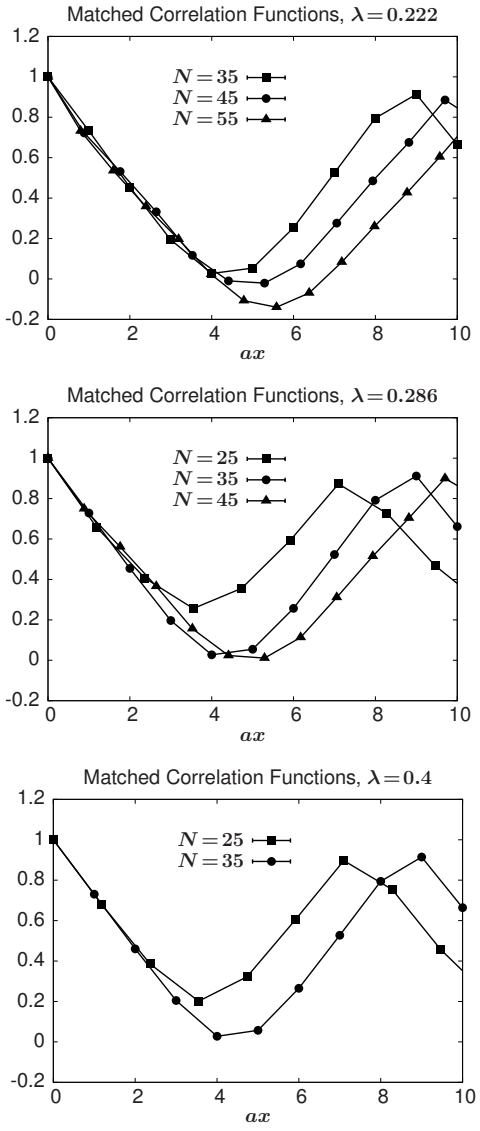

Figure 8: Examples of "matched correlation functions": at different system sizes N and at fixed coupling λ, $\Delta m^2 = m^2 - m_c^2$ is tuned such that the short-distance correlations agree. Then the distance in physical units — as given in eq. (4.3) — agrees as well. Thus we identify the Δm^2 values to be inserted in eq. (4.5), which fixes the critical exponent σ. (Again the correlation functions are normalised to 1 at $x = |\vec{x}| = 0$.)

the DSL. Table 1 and Figure 9 show our results, which explore the window of sizes and couplings, which are numerically well tractable.

λ	N_1	m^2	m_c^2	N_2	m^2	m_c^2	σ
0.222	35	-0.59	$-0.60(3)$	45	-0.77	$-0.83(4)$	0.152(7)
	35			55	-0.84	$-0.99(4)$	0.156(6)
	45	-0.77	$-0.83(4)$	55			0.161(11)
0.286	25	-0.59	$-0.63(2)$	35	-0.66	$-0.85(3)$	0.161(9)
	25			45	-0.57	$-1.03(5)$	0.167(7)
	35	-0.66	$-0.85(3)$	45			0.178(23)
0.4	25	-0.88	$-0.95(5)$	35	-0.91	$-1.25(7)$	0.147(13)

Table 1: The σ-values obtained for various pairs of sizes N_1, N_2 after tuning Δm^2 such that the short-distance decay of the correlation functions coincide.

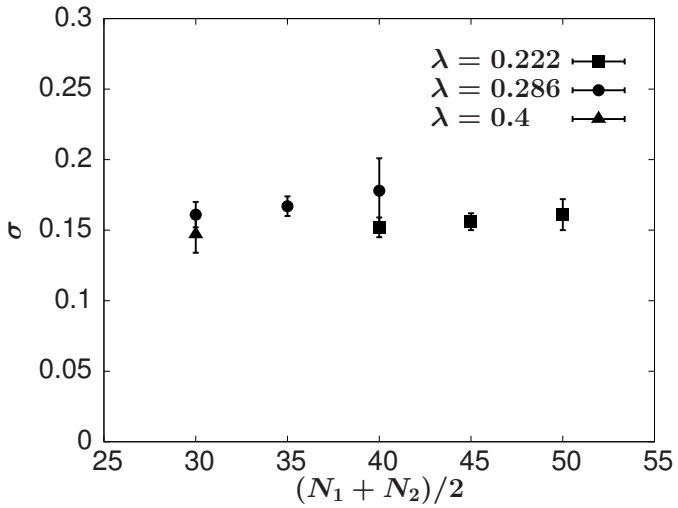

Figure 9: An illustration of the values given in Table 1. There is a clear trend to a plateau value of $\sigma = 0.16(1)$.

We see a convincing trend towards a stable critical exponent

$$\sigma = 0.16(1) \ . \tag{4.6}$$

Therefore our results give evidence for the persistence of the striped phase in the DSL.

5 Conclusions

We have presented a non-perturbative, numerical study of the $\lambda\phi^4$ model on a NC plane. Regularising the model as a lattice theory, and mapping the latter to a matrix formulation, enabled us to determine the phase structure of this model by means of Monte Carlo simulations, without relying on weak- or strong-coupling assumptions.

Our study of the phase diagram of the lattice model at finite lattice spacing reveals the existence of phases corresponding to disorder, uniform order and non-uniform order, in agreement with expectations based on analytical studies, and with previous numerical work on this and in related models. In particular, the typical configurations in the non-uniform order phase are characterised by spontaneous breaking of rotational and translational symmetries, with patterns of separated regions, in which the field takes different values ("stripes"). This phase is absent in the commutative case.

The three different phases are separated by transition lines, which stabilise rapidly when the system size N is increased, if the axes are scaled suitably — that prescription differs from the 3d case.

In order to define a "physical" value for the lattice spacing a and take the continuum limit (at fixed non-commutativity parameter), we have introduced a dimensional scale based on the decay of the correlation function (although this decay is not exponential). This allows us to identify trajectories in the parameter space, which can be extrapolated to the DSL, *i.e.* to the continuum and to infinite volume, at a constant NC parameter θ.

We have provided evidence that a DSL can be taken in the vicinity of the striped phase, which means that this exotic phase does persist in the continuum and in infinite volume. This implies in particular that the spontaneous breaking of translation and rotation symmetry occurs. The apparent contradiction with the Mermin-Wagner theorem is avoided by the fact that this model is non-local, and that its IR behaviour is not smooth.

Acknowledgements We are indebted to Frank Hofheinz for his help with the design of the figures. We also thank him, as well as Jan Ambjørn, Antonio Bigarini, Steven Gubser, Jun Nishimura, Denjoe O'Connor and Jan Volkholz for useful communications. This work was supported by the Mexican *Consejo Nacional de Ciencia y Tecnología* (CONACyT) through project 155905/10 "Física de Partículas por medio de Simulaciones Numéricas", and by the Spanish *MINECO* (grant FPA2012-31686 and "Centro de Excelencia Severo Ochoa" programme grant

SEV-2012-0249). The simulations were performed on the cluster of the Instituto de Ciencias Nucleares, UNAM.

A Numerical techniques

In the formulation that we simulated, a configuration is given by a Hermitian $N \times N$ matrix Φ, where N is odd, cf. Section 2. We applied the standard Metropolis algorithm, and proceeded with local, Hermiticity-preserving, updates of the matrix elements, $\Phi_{ij} \to \Phi'_{ij}$, $\Phi_{ji} \to \Phi^{'}_{ij}{}^{*}$.

In this appendix we comment on a numerically efficient treatment of the action (2.2),

$$\begin{aligned} S[\Phi] &= N \ \mathrm{Tr} \ \left[\frac{1}{2} \sum_{\mu=1}^{2} (\Gamma_\mu \Phi \Gamma_\mu^\dagger - \Phi)^2 + \frac{\bar{m}^2}{2} \Phi^2 + \frac{\bar{\lambda}}{4} \Phi^4 \right] \\ &:= N \left[\frac{1}{2} (s_{\mathrm{kin},1} + s_{\mathrm{kin},2}) + \frac{\bar{m}^2}{2} s_m + \frac{\bar{\lambda}}{4} s_\lambda \right] \ . \end{aligned} \tag{A.1}$$

The twist eaters Γ_μ are given in Section 2; note that the diagonal elements of Γ_2 are powers of $z = -e^{-\,\mathrm{i}\,\pi/N}$.

To discuss the evaluation of these terms, we mention that any Hermitian matrix H fulfils

$$\mathrm{Tr}\, H^2 = \sum_{ij} |H_{ij}|^2 = \sum_i H_{ii}^2 + 2 \sum_{i>j} |H_{ij}|^2 \ . \tag{A.2}$$

- We first address $s_{\mathrm{kin},1}$, where it is useful to introduce the notation

$$\bar{i} := i \ \mathrm{mod} \ N \tag{A.3}$$

The matrix $\Gamma_1 \Phi \Gamma_1^\dagger - \Phi$ is also Hermitian, hence we apply the identity (A.2) to arrive at the computationally economic form

$$s_{\mathrm{kin},1} = \sum_i (\Phi_{\overline{i+1},\, \overline{i+1}} - \Phi_{ii})^2 + 2 \sum_{i>j} |\Phi_{\overline{i+1},\, \overline{j+1}} - \Phi_{ij}|^2 \ . \tag{A.4}$$

- For the $s_{\mathrm{kin},2}$ term, note that

$$(\Gamma_2 \Phi \Gamma_2^\dagger)_{ij} = \Phi_{ij} z^{i-j} \tag{A.5}$$

is still Hermitian, and $\Gamma_2 \Phi \Gamma_2^\dagger - \Phi$ as well. Inserting z yields

$$\begin{aligned} s_{\mathrm{kin},2} &= \sum_{ij} \left| \Phi_{ij} \left(z^{i-j} - 1 \right) \right|^2 \\ &= 4 \sum_{i>j} |\Phi_{ij}|^2 \ \left[1 - (-1)^{i-j} \cos \frac{\pi(i-j)}{N} \right] \ . \end{aligned} \tag{A.6}$$

• There are also simplifications of the action difference, which is needed in the Metropolis accept/reject step. For

$$\Delta s_{\mathrm{kin}} := s_{\mathrm{kin},1}[\Phi'] + s_{\mathrm{kin},2}[\Phi'] - s_{\mathrm{kin},1}[\Phi] - s_{\mathrm{kin},2}[\Phi] \ . \tag{A.7}$$

we obtain

$$\begin{aligned} \Delta s_{\mathrm{kin}}(i=j) &= 2 \Big[{\Phi'_{ii}}^2 - \Phi_{ii}^2 + (\Phi_{ii} - \Phi'_{ii}) \, (\Phi_{\overline{i+1},\, \overline{i+1}} + \Phi_{\overline{i-1},\, \overline{i-1}}) \Big] \\ \Delta s_{\mathrm{kin}}(i \neq j) &= 4 \Big[(|\Phi'_{ij}|^2 - |\Phi_{ij}|^2) \left(2 - \cos \frac{(N+1)\pi(i-j)}{N} \right) \\ &\quad + \mathrm{Re} \left((\Phi_{ij} - \Phi'_{ij}) \, (\Phi_{\overline{i+1},\, \overline{j+1}} + \Phi_{\overline{i-1},\, \overline{j-1}}) \right) \Big] \ . \end{aligned} \tag{A.8}$$

The cosine function in this formula, and in eq. (A.6), is only required for $(N-1)$ different arguments, which should be stored in a look-up array.

• The *mass term* $s_m = \mathrm{Tr}\, \Phi^2$ is quick to evaluate, thanks to identity (A.2). The main computational challenge is the *quartic term*

$$s_\lambda = \mathrm{Tr}\, \Phi^4 = \sum_r (\Phi^2)_{rr}^2 + 2 \sum_{r>s} |(\Phi^2)_{rs}|^2 \ . \tag{A.9}$$

When updating a generic matrix element Φ_{ij}, $i \geq j$, the difference Δs_λ is affected by the following elements of Φ^2,

$$(\Phi^2)_{is} \ \text{ for } \ s = i \ldots N \ , \quad (\Phi^2)_{rj} \ \text{ for } \ r = 1 \ldots j \ . \tag{A.10}$$

These elements have to be computed explicitly for Φ^2 and for ${\Phi'}^2$. A final detail is that the elements for the same indices r, s — belonging to the set specified in (A.10) — can be obtained without doing the full summation twice, since most contributions are identical,

$$({\Phi'}^2)_{rs} = (\Phi^2)_{rs} + \begin{cases} |\Phi'_{ij}|^2 - |\Phi_{ij}|^2 & \text{if} \quad r = s \\ (\Phi'_{ij} - \Phi_{ij}) \Phi_{js} & \text{if} \quad i = r \neq s \\ \Phi_{ri} (\Phi'_{ij} - \Phi_{ij}) & \text{if} \quad j = s \neq r \end{cases} \ . \tag{A.11}$$

References

[1] M.R. Douglas and N.A. Nekrasov, *Rev. Mod. Phys.* **73** (2001) 977.

[2] R.J. Szabo, *Phys. Rep.* **378** (2003) 207.

[3] H.S. Snyder, *Phys. Rev.* **71** (1947) 38.

[4] N. Seiberg and E. Witten, *JHEP* 09 (1999) 032.

[5] S. Minwalla, M. Van Raamsdonk and N. Seiberg, *JHEP* **02** (2000) 020.

[6] S.S. Gubser and S.L. Sondhi, *Nucl. Phys.* **B 605** (2001) 395.

[7] G.-H. Chen and Y.-S. Wu, *Nucl. Phys.* **B 622** (2002) 189.

[8] P. Castorina and D. Zappalà, *Phys. Rev.* **D 68** (2003) 065008. J.M. Hernández, C. Ramírez and M. Sánchez, *Phys. Rev.* D **87** (2013) 125012.

[9] W. Bietenholz, F. Hofheinz and J. Nishimura, *Nucl. Phys. (Proc. Suppl.)* **119** (2003) 941; *JHEP* **0406** (2004) 042. F. Hofheinz, Ph.D. thesis, Humboldt Universität zu Berlin (2004) [`hep-th/0403117`].

[10] J. Ambjørn and S. Catterall, *Phys. Lett.* **B 549** (2002) 253.

[11] D. Mermin and H. Wagner, *Phys. Rev. Lett.* **17** (1966) 1133. P.C. Hohenberg, *Phys. Rev.* **158** (1967) 383. S.R. Coleman, *Commun. Math. Phys.* **31** (1973) 259.

[12] P. Castorina and D. Zappalà, *Phys. Rev.* **D 77** (2008) 027703.

[13] H. Mejía-Díaz, B.Sc. thesis, Universidad Nacional Autónoma de México, 2013. W. Bietenholz, F. Hofheinz, H. Mejía-Díaz and M. Panero, arXiv:1402.4420 [hep-th].

[14] A. González-Arroyo and M. Okawa, *Phys. Lett.* **B 120** (1983) 174.

[15] W. Bietenholz, F. Hofheinz and J. Nishimura, *JHEP* **0209** (2002) 009; W. Bietenholz, J. Nishimura, Y. Susaki and J. Volkholz, *JHEP* **0610** (2006) 042; W. Bietenholz, A. Bigarini and A. Torrielli, *JHEP* **0708** (2007) 041.

[16] B. Lucini and M. Panero, *Phys. Rept.* **526** (2013) 93.

[17] M. García Pérez, A. González-Arroyo and M. Okawa, *JHEP* **1309** (2013) 003.

[18] J. Ambjørn, Y.M. Makeenko, J. Nishimura and R.J. Szabo, *JHEP* **11** (1999) 29; *Phys. Lett.* **B 480** (2000) 399; *JHEP* **05** (2000) 023.

[19] H. Aoki, N. Ishibashi, S. Iso, H. Kawai, Y. Kitazawa and T. Tada, *Nucl. Phys.* **B 565** (2000) 176.

[20] H. Steinacker, *JHEP* **0503** (2005) 075.

[21] X. Martin, *JHEP* **0404** (2004) 077. M. Panero, *SIGMA* **2** (2006) 081; *JHEP* **0705** (2007) 082. F. García Flores, X. Martin and D. O'Connor, *Int. J. Mod. Phys.* **A 24** (2009) 3917. B. Ydri, *JHEP* **1403** (2014) 065.

[22] J. Medina, Ph.D. thesis, CINVESTAV (Mexico D.F.) 2006 [arXiv:0801.1284 [hep-th]]. J. Medina, W. Bietenholz and D. O'Connor, *JHEP* 0804 (2008) 041.

[23] S. Digal, T.R. Govindarajan, K.S. Gupta and X. Martin, arXiv:1109.4014 [gr-qc].

[24] Y. Shimamune, *Phys. Lett.* **108 B** (1982) 407.